IMAGE AND SHAPE RECONSTRUCTION IN ELECTRICAL RESISTANCE TOMOGRAPHY

M. Soleimani*, and A. Movafeghi**

* William Lee Innovation Centre, school of materials, the University of Manchester , UK
** NDT Dept., Radiation Protection Tech. Centre, AEOI, Tehran, Iran

M.Soleimani-2@manchester.ac.uk , amovafeghi@gmail.com

Abstract: Electrical resistance tomography (ERT) has great potential to be used for multi-phase flow monitoring. The Image reconstruction in ERT is computationally costly, so the online monitoring is a difficult task. The linear reconstruction methods are currently used as fast methods. The image reconstruction is a nonlinear inverse problem and the linear methods are not sufficient in many cases. The application of a recently proposed non-iterative inversion method for two-phase materials in has been studied. The method works based on Monotonicity property of the resistance matrix in ERT and it requires modest computational cost. In this paper we explain the application of this inversion method. We demonstrate the capabilities and drawbacks of the method by using 2D test examples. A major contribution of this paper is to optimize the software program for the inversion (by doing most of the computations offline), so it can be used for online application.

Introduction

Electrical resistance tomography (ERT) is relatively new imaging modality [1]. ERT attempts to reconstruct the conductivity distribution inside a material. The ERT data is a set of the measurements of the DC resistances between pairs of electrodes in contact with the conductor under investigation. Figure 1 is a picture of the experimental ERT system, designed and fabricated in Sharif University of technology [2].

There are many applications that ERT system is to image an interface between two-phase materials. In such cases the objective of the image reconstruction is to identify the shape of inclusions. In this paper we present a shape reconstruction technique for ERT based on montonicity property of the resistance matrix [2]. is the official language. Please, do not forget to check the spelling. Read the instructions in this sample abstract carefully before typing.

Materials and Methods

The block-diagram of SUT-1 [6], is shown in Figure 1. Here only the main blocks of system hardware are discussed. Moreover, for each measuring channel, a well-known block is used [3]. The utilized computer is a usual Pentium-base PC, which is connected to the measurement system through an Input-Output interface (I/O) card. In the main board a current generator with 5mA @ 23 kHz and a precision voltage measurement (using synchronized pulse demodulation technique) are implemented. The accuracy of digital system is 12 bits. It is shown that the 12-bit digital resolution is a reasonable choice for the most applications [2]. The switching between different pairs of electrodes is carried out by computer using multiplexer card (MUX board). The collected data from all possible voltage measurements are fed to the image reconstruction software. In the following a brief description of any individual module of this system is shown.

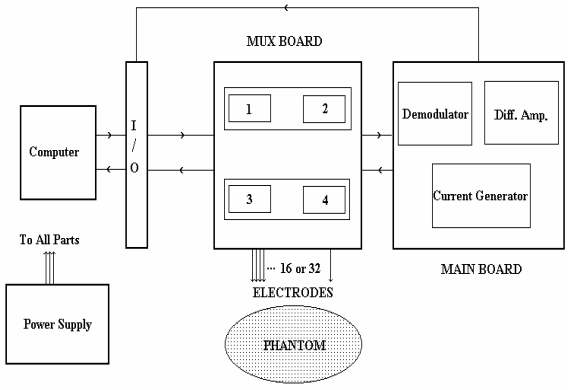

Figure 1: The block- diagram of SUT-1

I/O card: For I/O module, an ADVANTECH PCL-812PG I/O card is used [13]. It consists of 16 bit programmable I/O card with 12-bit successive approximation analogue to digital converter, (30 kHz sampling rate), programmable Time/Counter/Gain and two 12 bit monolithic multiplying digital to analogue converter output channels. Due to application of an unsophisticated analogue to digital conversion algorithm, it is not a fast sampling card.

Forward model: The mathematical model of ERT, assuming a linear material of conductivity σ and the complete electrode model [3],[4],[5], which includes a contact resistance z_k between the electrodes and the conductor, is given by

$$\nabla \cdot (\sigma \nabla \phi) = 0 \quad \text{in } V_c \qquad (1)$$

$$\phi + z_k \sigma \frac{\partial \phi}{\partial \nu} = V_k, \; k = 1, \ldots, N$$

Where V_k is the potential applied to the *k-th* electrode, V_c is the conductive domain, σ is the conductivity, ϕ is the scalar potential and N is the

ISSN: 1727-1983

number of electrodes. The current i_k flowing into the conductor through the k-th electrode is given by $I_k = \int_{E_i} \sigma \frac{\partial \phi}{\partial \nu} ds$.

Figure 2 shows an electric potential distribution from our forward solver using finite element method. In figure 3 one can see a set of resistance measurement.

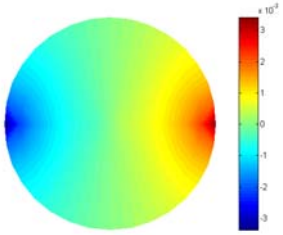

Figure 2: Electric potential distribution with opposite current pattern

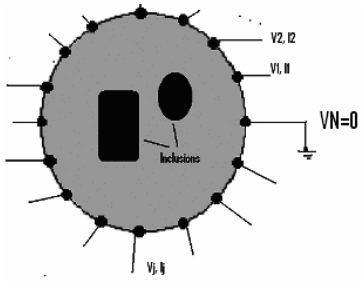

Figure 3: Measurement of the resistance matrix

Thanks to the linearity of the model, the relation between electrodes currents and voltages is given by a matrix multiplication **v=Ri** , Where **R** is the resistance matrix, an (N-1)(N-1) symmetric matrix, **v** and **i** are the columns vectors of electrodes voltages and currents, respectively. corresponding measured voltages is shown at right.

We notice that usual measurements protocol does not directly measure the resistance matrix. In these cases, the resistance matrix can be easily recovered from the measured data (assuming that N(N-1)/2 measurements are available). The main property of the resistance matrix, from the perspective of the inversion method, is the monotonicity, see [4].

$$\eta_1(\mathbf{x}) \geq \eta_2(\mathbf{x}) \text{ in } V_c \Rightarrow \mathbf{R}_1 \geq \mathbf{R}_2 \qquad (2)$$

Where $\mathbf{R}_k$ is the second order moment associated η_k. For two phases problem, (2) can be recast as

$$D_\beta \subseteq D_\alpha \subseteq V_c \Rightarrow \mathbf{R}_\alpha \geq \mathbf{R}_\beta \qquad (3)$$

Where $\mathbf{R}_\gamma$, for $\gamma \in \{\alpha, \beta\}$ is the resistance matrix related to a resistivity η_γ defined as

$$\eta_\gamma(\mathbf{x}) = \begin{cases} \eta_i & \forall \mathbf{x} \in D_\gamma \\ \eta_b & \forall \mathbf{x} \in V_c / D_\gamma \end{cases}$$

Where η_b is the resistivity of the first phase that we call the background phase, and $\eta_i > \eta_b$ is the resistivity of the second phase that we call inclusion or anomalous phase. We stress that the monotonicity (2) and (3) hold for the actual resistance matrix and for the numerically computed resistance matrix.

Inversion algorithm: The inversion method here presented for two-phase problems, is a quantitative non-iterative inversion method [4] requiring the solution of a number of direct problems growing as O(N), where N is the number of voxels used to discretize the unknown. In the following we briefly summarize the inversion method with reference to the ERT. The inversion method is based on the following property of the unknown-data mapping

$$D_\beta \subseteq D_\alpha \subseteq V_c \Rightarrow \mathbf{R}_\alpha - \mathbf{R}_\beta \text{ is a positive semi-definite matrix} \qquad (4)$$

Reversing (4) we obtain the proposition at the basis of the inversion method:

$$\mathbf{R}_\alpha - \mathbf{R}_\beta \text{ not a positive semi-definite matrix} \Rightarrow D_\beta \not\subseteq D_\alpha \qquad (5)$$

Proposition (5) is a criterion allowing us to exclude the possibility that D_β is contained in D_α using from the resistance matrices $\mathbf{R}_\alpha$ and $\mathbf{R}_\beta$. Notice that (5) does not exclude that D_α and D_β are overlapped, i.e. does not exclude the case $D_\beta \cap D_\alpha \neq \varnothing$ where $\varnothing$ is the void set.

Let us initially assume that the measured resistance matrix $\tilde{\mathbf{R}}$ is noise free ($\tilde{\mathbf{R}}$ corresponds to the anomaly in V), that the conductive domain V_c is divided into N "small" non-overlapped parts $\Omega_1,\ldots,\Omega_N$ and that the anomalous region V is union of some Ω_k's (figure 4).

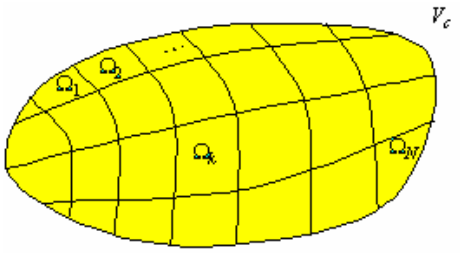

Figure 4: Dividing to pixels

The proposition (5) yields in a rather natural inversion method. In fact, to understand if a given Ω_k is part of V (given the knowledge of $\tilde{\mathbf{R}}$) we need to compute the largest positive and the smallest negative eigenvalues of the matrix $\tilde{\mathbf{R}} - \mathbf{R}_k$, where $\mathbf{R}_k$ is the resistance matrix corresponding to an anomalous region in Ω_k If the product of these two eigenvalues is negative, then $\tilde{\mathbf{R}} - \mathbf{R}_k$ is not a positive semi-definite matrix and, therefore, from (5) applied to $\tilde{\mathbf{R}}$ and $\mathbf{R}_k$ it follows

ISSN: 1727-1983

that $\Omega_k \not\subseteq V$. Since Ω_k is contained in V or external to V (we are assuming that V is union of some Ω_k's), it follows that Ω_k cannot be included in V. It is worth noting that the criterion (5) is a sufficient condition to exclude Ω_k from V. Therefore, the reconstruction $\tilde{V}$ obtained as the union of those Ω_k such that $\tilde{\mathbf{R}} - \mathbf{R}_k$ is positive semi-definite includes V, i.e. $V \subseteq \tilde{V}$.

In addition, we notice that the test matrices $\mathbf{R}_1, \ldots, \mathbf{R}_N$ can be precomputed and easily stored since they are $N_e \times N_e$ symmetric matrices, where N_e is the number of electrodes (apart from the reference electrode) that, generally, is a number not exceeding few dozens. In addition, the computational cost to compute the largest and smallest eigenvalues of $\tilde{\mathbf{R}} - \mathbf{R}_k$ is moderate. The method is non-iterative we can decide if Ω_k is part of V independently from Ω_i for $i \neq k$.

Once the exterior set is defined, the second test can be used to find the interior set. The combination of the test results allows the shape of the inclusions to be approximately determined. Those pixels in the interior set are definitely in the inclusions, those not in the exterior sets are definitely not in inclusions. It is not possible, however, to definitively assign the remaining pixels. Further modelling will be introduced before an attempt is made to assign these pixels.

Results

For this part, we measured the voltage and then reconstructed images in 16 and 32 electrodes modes. In practical conditions, EIT is very sensitive to noise. Electrodes are connected via a shielded cable to the system for noise reduction. Figures 5-6 illustrate two actual images using a phantom in experimental EIT system [2]. The phantom was made of PVC cylinder with 30 cm diameter and filled with saline. Figure 6 shows the design and experimental results for a phantom where an object with different resistivity (a normal milk bottle) is put at the corner, i.e., at x=0 cm and y=-6 cm from the geometrical center of the tank. Figure 5 shows the design and experimental results for a phantom with two objects. Measured data were transferred to the computer, the reconstruction algorithm applied and image was obtained using back projection method.

As seen in Figure 6, a star artifact is resulted from back projection. This is a well-known artifact for the back projection method. Basically, it is due to limitation in the number of projections.

Figure 7 shows reconstruction of shape (in left), where area including gray and white in figure 6 (right) is the result of the exclusion test. The white area in figure 6 is the resulting shape of inclusion by exclusion test.

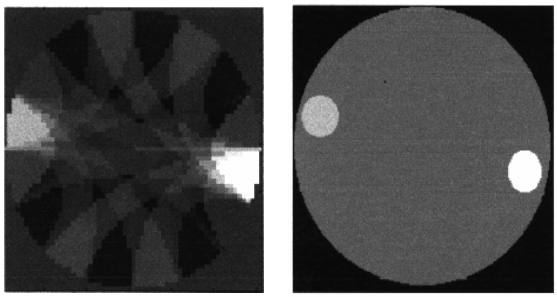

Figure 5: A real test object and its EIT reconstructed image using back projection method.

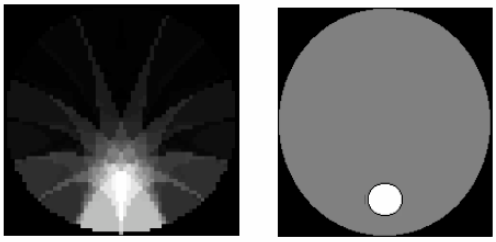

Figure 6: Another real test object and its EIT reconstructed image using back projection method.

Figure 7: True image (left), reconstructed (right)

Figure 8 and 9 show reconstruction of the shape of an inclusion in 12 two electrodes EIT arrangement a circular cross section (to represent cross section of a pipe line) and a rectangular shape (represent the .

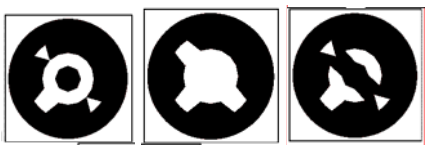

Figure 8: True image (left), exterior test (middle), interior test (right)

ISSN: 1727-1983

Figure 9: True image (left), reconstructed (right)

For the monotonicity technique one needs to solve N forward problem (for each inverse pixel), for the excluding test. This can be done offline as the method assumes two phase materials and the conductivity of two phases are known. The inclusion test requires fewer number of the forward solution and can be done online. (see figure 10)

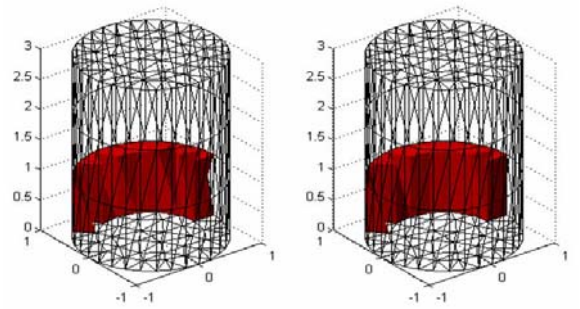

Figure 10: Shape reconstruction, the inclusion of test in left reconstructed in right.

Conclusions

The monotonicity method potentially offers a fast, stable, non-iterative, and non-linear reconstruction algorithm for the important use of two-phase mixtures in resistance tomography. The method has been tested for 2D test examples in this paper. A major part of the computations (solving the forward problems for the excluding test) can be done offline, so the technique can potentially be used for online applications. In practice, back projection as a fast inverse solver produce low quality images. Other fast solver such as Landweber linear iterative method are working better than back projection, but suffering from a linearization assumption.

References

[1] Soleimani M. (1999): 'Design and fabrication a 32 electrodes electrical impedance tomography ', MSc thesis, Sharif University of Technology, Tehran

[2] Woo E., Hua P., Webster J. G and Tompkins W. J., (1993): 'A Robust Image Reconstruction Algorithm and Its Implementation in EIT', IEEE Trans. Med Imag., **12**, pp. 137-146

[3] Paulson K., Breckon W. and Pidcock. M. (1993): 'Electrode Modeling In Electrical-Impedance Tomography', Siam J. of Appl. Math.', **52**, pp. 1012-1022

[4] E Sommersalo, M. Cheney and D. Isaacson., (1993): 'Existence and Uniqueness for an Electrode Model for ECT', Siam J. of Appl. Math., **52**, pp. 1023-1040

[5] A., Tamburrino A. and G. Rubinacci., (2002): 'A new non-iterative inversion method in electricalresistance tomograph', Inverse Problems, 18, pp.1809-1829,

[6] M. Soleimani, A. Movafeghi, (2005): 'Electrical resistance tomography: a shape reconstruction method for two phase materials', Int. J. Sci. Res. **15** (to appear)

ISSN: 1727-1983